

## Supplementary Information

### Highly efficient UV-visible-infrared light-driven photothermocatalytic steam biomass reforming to H<sub>2</sub> on mesoporous silica loaded Ni nanoparticles

Chongyang Zhou, Jichun Wu, Yuanzhi Li\*, Huamin Cao

State Key Laboratory of Silicate Materials for Architectures (Wuhan University of Technology), 122 Luoshi Road, Wuhan 430070, P. R. China. Email: [liyuanzhi@whut.edu.cn](mailto:liyuanzhi@whut.edu.cn)

#### Methods

**Reagents.** Concentrated HNO<sub>3</sub> (68 wt%), Na<sub>2</sub>SiO<sub>3</sub>·9H<sub>2</sub>O, Ni(NO<sub>3</sub>)<sub>2</sub>·6H<sub>2</sub>O, concentrated ammonia (25~28 wt%) were purchased from Sinopharm Chemical Reagent Co., Ltd. Cellulose, D<sub>2</sub>O, and H<sub>2</sub><sup>18</sup>O were purchased from Aladdin. Agricultural wastes of rice straw, wheat straw, and corn stalk were collected from a local farmer at Suizhou, Hubei province, China. Kitchen waste was collected from the author's family. The reagents were used as received without further purification.

**Catalyst preparation.** The sample of nickel nanoparticles loaded on mesoporous silica was prepared according to the following procedure. 25.5798 g of Na<sub>2</sub>SiO<sub>3</sub>·9H<sub>2</sub>O was dissolved in 84 mL deionized water in a beaker. A HNO<sub>3</sub> aqueous solution, obtained by diluting concentrated HNO<sub>3</sub> with deionized water according to a volume ratio of 1: 4, was dropped to the Na<sub>2</sub>SiO<sub>3</sub> aqueous solution under magnetic stirring until the pH value was about 6. A Ni(NO<sub>3</sub>)<sub>2</sub> aqueous solution, obtained by dissolving 1.3774 g of Ni(NO<sub>3</sub>)<sub>2</sub>·6H<sub>2</sub>O in 10 mL deionized water, was dropped to the resultant silica sol-gel under magnetic stirring. 6.0 mL of diluted ammonia aqueous solution, obtained by diluting concentrated ammonia solution with deionized water according to a volume ratio of 1:5, was dropped to the mixture under magnetic stirring. The beaker, covered with polyethylene film, was heated at 90 °C for 24 h in an electric oven. The precipitate was filtered, washed with deionized water, and dried at 180 °C for 24 h. The obtained NiO/SiO<sub>2</sub> sample, placed in a quartz tubular reactor, was reduced at 700 °C for 2 h in a flow of pure H<sub>2</sub>. The obtained sample was labeled as Ni/m-SiO<sub>2</sub>.

The referenced sample of mesoporous silica (labeled as SiO<sub>2</sub>) was prepared according to the same procedure as the NiO/SiO<sub>2</sub> sample except for no adding Ni(NO<sub>3</sub>)<sub>2</sub> aqueous solution.

**Characterization.** XRD pattern of Ni/m-SiO<sub>2</sub> was obtained from a Rigaku D/max diffractometer with Cu K $\alpha$  radiation. TEM images were collected on a JEM-100CX transmission electron microscope.

The specific surface area and pore volume were measured on an ASAP2020 instrument using N<sub>2</sub> absorption at -196 °C. The compositions of the agricultural wastes and kitchen wastes were analyzed on a Vario EL cube Elementar (Supplementary Table S1). The amount of char produced by the catalytic biomass reforming and the total amount of organic compounds in the wastes were determined by TG-MS on a HCT-1 thermal analyzer linked with a QMS403 mass spectrometer in a flow of air. The diffuse reflectance absorption spectra were recorded on a Lambda 750 spectrophotometer. FTIR spectra were recorded on a Nicolet 6700 IR spectrometer.

**Photothermocatalytic or photocatalytic test.** The photothermocatalytic steam biomass reforming and cellulose pyrolysis on the samples merely with the focused illumination from a 500 W lamp was evaluated on a setup (Supplementary Scheme S1) by using a photothermocatalytic reactor (Fig. 2a). 0.8080 g cellulose and 0.0807 g of the catalyst were ground in an agate mortar. 1.5010 g deionized water was added, and ground to a homogeneous mixture. 0.1443 g of the mixture was placed in an alumina crucible which was supported by insulation aluminum silicate fibers in the reactor. Before the reaction, the reactor was evacuated by a vacuum pump. Then, the illumination from the Xe lamp was focused on the mixture. After being illuminated for nine minutes, the Xe lamp was switched off. High-purity Ar was filled in the reactor until the inner pressure reached atmospheric pressure. The produced gases, such as H<sub>2</sub>, CO, CO<sub>2</sub>, and CH<sub>4</sub> were analyzed by a GC9560 gas chromatograph. The details of GC analysis and the measurement of light intensity were reported in the previous work<sup>s1</sup>. The photothermocatalytic test was repeated three times. The catalytic data of the sample were the average value of the three times tests. To measure the photothermocatalytic activity of the sample with focused vis-IR illumination, a long-wave pass cut-off filter of  $\lambda > 420$  or 560 nm was placed on the quartz window of the reactor. The power values ( $P$ ) of the illumination focused into the reactor with the UV-vis-IR,  $\lambda > 420$  nm, and  $\lambda > 560$  nm illumination are 7088.4, 5948.2, and 5155.7 mW, respectively. As the size of the light spot was about 5 mm, their corresponding light intensity values are 361.0, 302.9, 262.6 KW m<sup>-2</sup>, respectively.

In principle, the light-to-fuel efficiency ( $\eta$ ) for photothermocatalytic steam cellulose reforming should be calculated by the equation as follows.

$$\eta = (r_{\text{CO}} \times \Delta_c H^0_{\text{CO}} + r_{\text{H}_2} \times \Delta_c H^0_{\text{H}_2} + r_{\text{CH}_4} \times \Delta_c H^0_{\text{CH}_4} + r_{\text{char}} \times \Delta_c H^0_{\text{char}} + r_{\text{tar}} \times \Delta_c H^0_{\text{tar}} - r_{\text{C}_6\text{H}_{10}\text{O}_5} \times \Delta_c H^0_{\text{C}_6\text{H}_{10}\text{O}_5}) \times m_{\text{catalyst}} / (P \times 3600)$$

$\Delta_c H^0_{\text{CO}}$ ,  $\Delta_c H^0_{\text{H}_2}$ ,  $\Delta_c H^0_{\text{CH}_4}$ ,  $\Delta_c H^0_{\text{char}}$ ,  $\Delta_c H^0_{\text{tar}}$ , and  $\Delta_c H^0_{\text{C}_6\text{H}_{10}\text{O}_5}$  are the standard combustion heats (298.15 K) of CO, H<sub>2</sub>, CH<sub>4</sub>, char, tar, and cellulose as fuels, respectively. CO<sub>2</sub> as a gas product is not fuel and its  $\Delta_c H^0_{\text{CO}_2}$  is 0.  $r_{\text{CO}}$ ,  $r_{\text{H}_2}$ ,  $r_{\text{CH}_4}$ ,  $r_{\text{char}}$ ,  $r_{\text{tar}}$ , and  $r_{\text{C}_6\text{H}_{10}\text{O}_5}$  (mmol g<sup>-1</sup> catalyst h<sup>-1</sup>) are the production rates of CO, H<sub>2</sub>, CH<sub>4</sub>, char, and tar as fuels, respectively.  $r_{\text{C}_6\text{H}_{10}\text{O}_5}$  is the reaction rate of the total consumed cellulose.  $P$  (mW) is the irradiation power focused illuminated into the reactor.  $m_{\text{catalyst}}$  is the weight (g) of the catalyst.

As the structure and composition of tar are very complicated and char is amorphous, it is difficult to get the accurate standard combustion heat values (298.15 K) of tar and char. Therefore, to simplify the  $\eta$  calculation, the following equation was used.

$$\eta = (r_{\text{CO}} \times \Delta_c H^0_{\text{CO}} + r_{\text{H}_2} \times \Delta_c H^0_{\text{H}_2} + r_{\text{CH}_4} \times \Delta_c H^0_{\text{CH}_4} + r_{\text{C}_6\text{H}_{10}\text{O}_5, \text{gas}} \times \Delta_c H^0_{\text{C}_6\text{H}_{10}\text{O}_5}) \times m_{\text{catalyst}} / (P \times 3600)$$

Where  $r_{\text{C}_6\text{H}_{10}\text{O}_5, \text{gas}}$  is the reaction rate of cellulose consumed to produce the gas products, which was calculated according to the following equations based the mass conversation of carbon.

$$r_{\text{C}_6\text{H}_{10}\text{O}_5, \text{gas}} = (C_{\text{CO}} + C_{\text{CO}_2} + C_{\text{CH}_4}) \times V / (24.45 \times 6 \times t \times m_{\text{catalyst}})$$

The production rate of the produced gas ( $r_i$ ,  $i = \text{H}_2$ , CO, CO<sub>2</sub>, and CH<sub>4</sub>) was calculated according to the following equation.

$$r_i = (c_i \times V) / (24.45 \times t \times m_{\text{catalyst}})$$

Where  $c_i$  is the volume concentration of the produced gas ( $i$ ).  $V$  is the volume (mL) of the reactor.  $t$  is the illumination time (h).  $m_{\text{catalyst}}$  is the weight (g) of the catalyst. Note: the volume of 1 mmol gas at room temperature (25 °C) is 24.45 mL.

For the isotope labeling test of photothermocatalytic cellulose reforming with D<sub>2</sub>O or H<sub>2</sub><sup>18</sup>O, the mixture was prepared by the same procedure as the mixture contained H<sub>2</sub>O described above except for using 0.3541 g D<sub>2</sub>O or H<sub>2</sub><sup>18</sup>O to replace H<sub>2</sub>O.

Rice straw, wheat straw, corn stalk, or kitchen waste was pulverized to small pieces by a home stainless pulverizer. The mixture for the photothermocatalytic steam biomass reforming was prepared by grinding the pulverized waste, the catalyst, and water according to the procedure described above. The amounts of biomass, the catalyst, and water in the mixture, and the amounts of the mixture used for photothermocatalytic steam biomass reforming are tabulated (Supplementary Table S2).

For the test of photocatalytic steam cellulose reforming on Ni/m-SiO<sub>2</sub> with focused UV-vis-IR illumination, the mixture was directly placed on the stainless bottom of the reactor. The reactor was laced in an ice-water bath to keep the temperature at near room temperature with the focused

UV-vis-IR illumination.

For photothermocatalytic steam biomass reforming, char and tar are produced as by-products, thus causing a reduction in the yield of the targeted gas products of H<sub>2</sub> and CO. Char is a solid of amorphous carbon due to the complete pyrolysis of biomass (e.g. cellulose complete pyrolysis: (C<sub>6</sub>H<sub>10</sub>O<sub>5</sub>)<sub>n</sub> = 6nC + 5nH<sub>2</sub>O). After the photothermocatalytic test, a solid mixture of the catalyst and char was remained in an alumina crucible in the reactor. The weight of char in the solid mixture was measured by TG-MS as described in Characterization.

The yield of char ( $y_{\text{char}}$ ) was calculated according to the following equation.

$$y_{\text{char}} (\%) = m_{\text{char}} / (m_i \times c_{i,C}) \times 100$$

Where  $m_{\text{char}}$  is the weight (g) of char.  $m_i$  is the weight (g) of the biomass (i) used for catalytic test, such as cellulose, rice straw, wheat straw, corn stalk, or kitchen waste.  $c_{i,C}$  is the weight ratio of carbon in the biomass.

$m_{\text{char}}$  was determined according to the following equation by measuring the weight loss ratio ( $r_{\text{wl}}$ , shown in Fig. S2a) of the remained solid mixture of the catalyst (Ni/m-SiO<sub>2</sub>) and the produced char after the photothermocatalytic test with TG-MS described in Characterization.

$$m_{\text{char}} = m_{\text{catalyst}} \times (r_{\text{wl}} + c_{\text{Ni}} \times m_{\text{O}} / m_{\text{Ni}}) / (1 - r_{\text{wl}})$$

Where  $c_{\text{Ni}}$  is the weight ratio of Ni in Ni/m-SiO<sub>2</sub>.  $m_{\text{O}}$  and  $m_{\text{Ni}}$  are the atomic weights of O and Ni, respectively.

Tar is a liquid mixture with higher boiling points. It has very complicated structures and compositions, which depend on the pyrolysis temperatures<sup>s2</sup>. Its formation is due to the very complicated reactions related to the partial pyrolysis of biomass (e.g. cellulose partial pyrolysis: (C<sub>6</sub>H<sub>10</sub>O<sub>5</sub>)<sub>n</sub> → C<sub>x</sub>H<sub>y</sub>O<sub>z</sub> + CO + H<sub>2</sub> + H<sub>2</sub>O + CO<sub>2</sub>). During the photothermocatalytic test, the formed tar was evaporated and mainly condensed on the quartz window of the reactor (*please see Fig. 2a*). This made the accurate collection of the formed tar very difficult. Therefore, the yield of tar ( $y_{\text{tar}}$ ) was obtained by the calculation according to the following equations based on the mass conversation of carbon.

$$y_{\text{tar}} (\%) = 100 - (c_{\text{CO}} + c_{\text{CO}_2} + c_{\text{CH}_4}) \times V \times 12 / (24450 \times m_i \times c_{i,C}) \times 100 - y_{\text{char}}$$

**Controlled catalytic test.** The catalytic steam cellulose reforming on Ni/m-SiO<sub>2</sub> with focused UV-vis-IR illumination or in the dark at different temperatures was evaluated on a set-up by using a tubular quartz reactor linked to a quartz window (Supplementary Scheme S2). The reaction temperature

was controlled by an electric tubular furnace. 0.0018 g of the mixture of cellulose, Ni/m-SiO<sub>2</sub> and water, prepared by the same procedure for the photothermocatalytic test described above, was placed in the reactor. Before the catalytic reaction, the reaction system was purged by a flow of high-purity Ar. The reactor was heated at a rate of 5 °C min<sup>-1</sup> to 750 °C in the dark or with the focused UV-vis-IR illumination. The light intensity of the focused UV-vis-IR illumination is 357.3 KW m<sup>-2</sup>.

For conducting the controlled catalytic cellulose pyrolysis on Ni/m-SiO<sub>2</sub> with focused UV-vis-IR illumination or in the dark at different temperatures, the mixture of cellulose and Ni/m-SiO<sub>2</sub> with a weight ratio of 10 was prepared by grinding cellulose and Ni/m-SiO<sub>2</sub>. The amount of the mixture was 0.0019 g. The other procedure was the same as that for the controlled catalytic steam cellulose reforming described above.

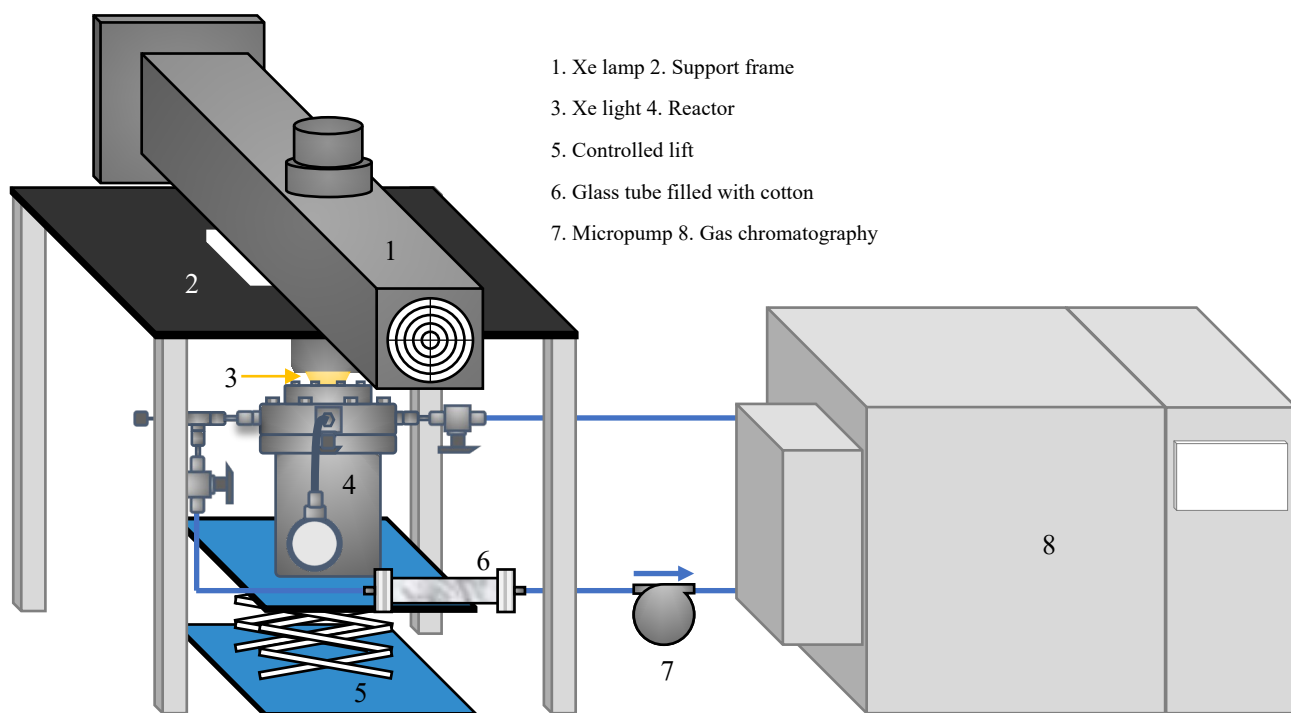
The controlled catalytic reaction between the pre-formed char on Ni/m-SiO<sub>2</sub> and water with focused UV-vis-IR illumination or in the dark at the different temperatures was conducted according to the following procedure. 0.0200 g of the mixture of cellulose and Ni/m-SiO<sub>2</sub> with a weight ratio of 10 was placed in the reactor. Before the catalytic reaction, the reaction system was purged by a flow of high-purity Ar. The reactor was heated at a rate of 5 °C min<sup>-1</sup> to 700 °C and kept at 700 °C for 30 min. After cooled to room temperature in the dark, 0.0190 g of the resultant Ni/m-SiO<sub>2</sub> sample with pre-formed char was mixed with 0.0500 g deionized water. 0.0019 g of the obtained mixture was placed into the reactor. The other procedure was the same as that for the controlled catalytic steam cellulose reforming.

**TPR.** H<sub>2</sub> temperature-programmed reduction (H<sub>2</sub>-TPR) in the dark and with illumination was performed on a TP5080 multifunctional adsorption apparatus using a quartz tube reactor, of which one end was linked to a quartz window. 0.0040 g of the Ni/m-SiO<sub>2</sub> sample was loaded in the reactor. The sample was heated to 700 °C at a rate of 10 °C min<sup>-1</sup> in a flow of pure H<sub>2</sub> with 24 ml min<sup>-1</sup> and kept at 700 °C for 2 hours. After cooled to room temperature, the H<sub>2</sub> gas was switched to a flow of 5 vol% O<sub>2</sub>/He and kept at room temperature for 30 min for oxygen chemisorption on Ni nanoparticles of Ni/m-SiO<sub>2</sub>. Then, the O<sub>2</sub>/He gas was switched to a flow of 5 vol% H<sub>2</sub>/Ar. The sample was heated from room temperature to 750 °C with 10 °C min<sup>-1</sup> in a flow of 5 vol% H<sub>2</sub>/Ar in the dark or with UV-vis-IR illumination.

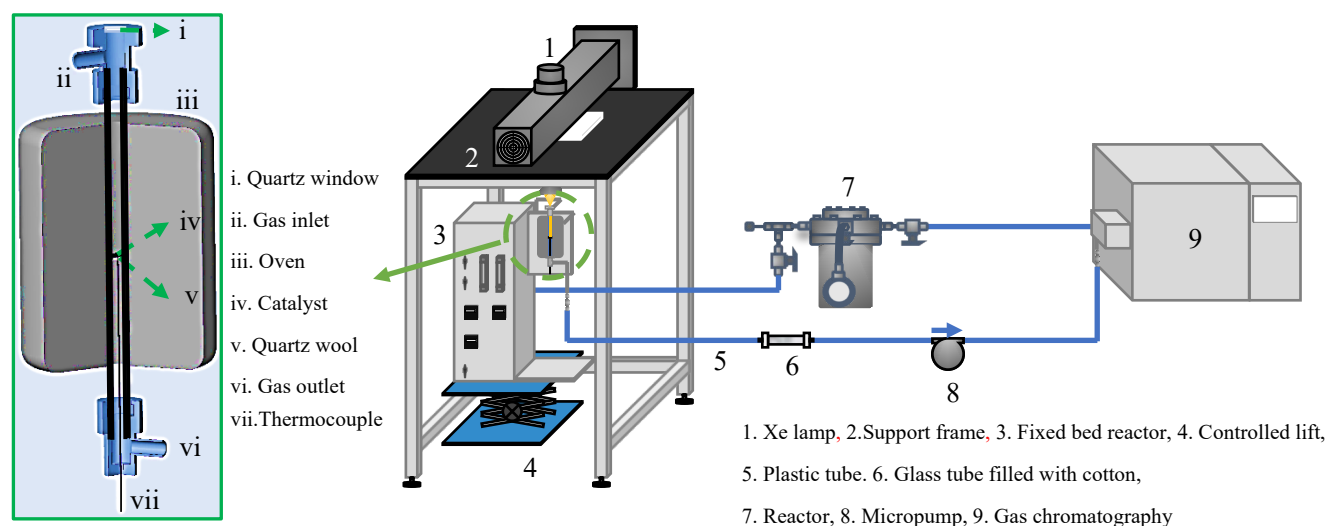
**DFT calculations.** Density functional theory (DFT) calculations were performed by Vienna Ab Initio Simulation Package (VASP 5.3). Perdew-Burke-Ernzerhof (PBE) GGA-exchange correlation

functional and Projected augmented wave (PAW) approach<sup>s3, s4</sup> is used. To simulate elementary steps of steam cellulose reforming on metallic nickel, a slab of Ni<sub>36</sub> with cubic structure (Ni: PDF 04-0850) and 3 × 3 {111} surface is constructed as the initial configuration. The space between neighbouring {111} surfaces in the slabs is 1.0 nm. The k-point mesh was 3 × 3 × 1 Monkhorst-Pack. The kinetic energy cutoff is 400 eV. The convergence criteria for ionic and electronic and relaxation are 10<sup>-3</sup> eV Å<sup>-1</sup> and 10<sup>-4</sup> eV, respectively.

The transition states of the elementary steps of steam cellulose reforming on the Ni<sub>36</sub> slab were searched by Dimer method<sup>s5, s6</sup>, in which a force-based conjugate gradient method is used<sup>s7</sup>. The convergence criteria for rotational force, and total energy and band structure energy are 0.01 eV Å<sup>-1</sup> and 1 × 10<sup>-7</sup> eV atom<sup>-1</sup>, respectively.



**Scheme S1.** Schematically illustrated set-up for measuring the photothermocatalytic activity of the samples for steam biomass reforming merely with focused illumination from a 500 W Xe lamp.



**Scheme S2.** Schematically illustrated set-up for measuring the catalytic activity of Ni/m-SiO<sub>2</sub> for cellulose steam reforming at the same temperature in the dark and merely with focused illumination from 500 W Xe lamp. *Note:* The reactor 7 in Scheme S2, in which no catalyst and cellulose were put, was used as a container for storing the gases produced by the reaction in the tubular quartz reactor.

**Table S1.** The compositions of the agricultural and kitchen wastes.

Substrates	The weight ratio (wt%)				Organic compounds
	C	H	N	S	
Rice straw	38.48	5.796	0.59	0.141	72.8
Wheat straw	41.24	6.027	0.51	0.070	71.4
Corn stalk	44.32	6.151	0.74	0.093	74.2
Dried kitchen waste*	42.39	5.747	2.52	0.227	9.7**

\* Dried kitchen waste was obtained by drying wet kitchen waste at 80 °C for 2h.

\*\* The data is the weight ratio of organic compounds in the wet kitchen waste.

**Table S2.** The amounts of biomass, the catalyst, and water in the mixture, and the amounts of the mixture used for photothermocatalytic steam biomass reforming tests.

	Amounts in the mixture (g)			Amount of the mixture (g)
	Biomass	Ni/m-SiO <sub>2</sub>	H <sub>2</sub> O	
Cellulose	0.808	0.0807	1.501	0.1443
Rice straw	0.1901	0.0139	0.9371	0.0811
Wheat straw	0.1943	0.0139	0.7945	0.0822
Corn stalk	0.1862	0.0138	0.7969	0.0802
Kitchen waste	1.4129	0.0136	0	0.1826

Note: as the pulverized kitchen waste contains a lot of water, no water was added in the mixture.

**Table S3.** The bond lengths of Ni-O for chemisorbed O and C on the Ni<sub>36</sub> slab in the ground state (Fig. S15g) and the excited state (Fig. S17g).

States	Bond	Bond length (Å)	
		In the ground state	In the excited state
Chemisorbed O and C	O-Ni (1)	1.84294	1.86013
	O-Ni (2)	1.78967	1.80236
	O-Ni (3)	1.84251	1.86267

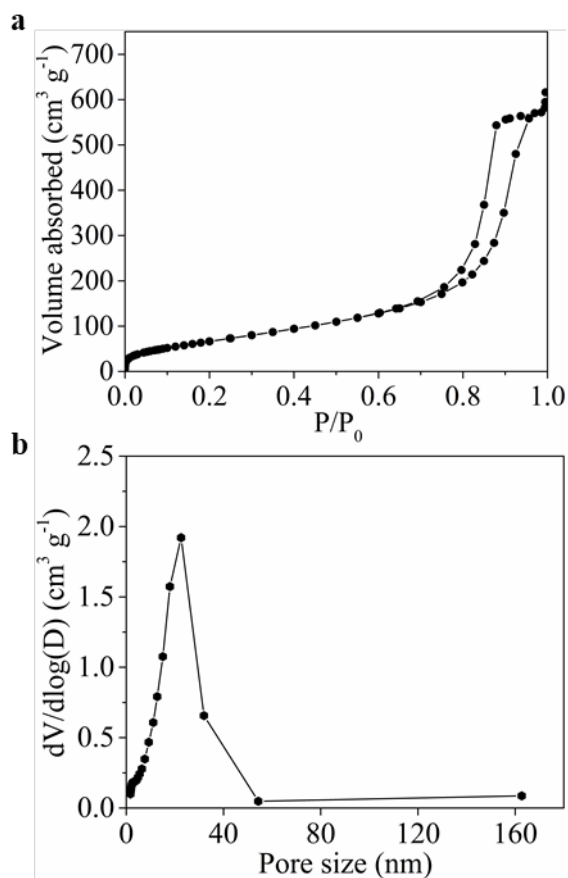


**Figure S1.** N<sub>2</sub> adsorption-desorption isotherm (a) and pore size distribution (b) of Ni/m-SiO<sub>2</sub>.

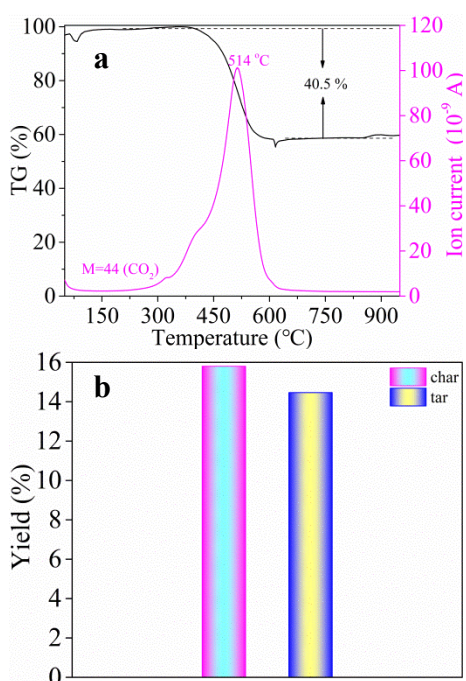


**Figure S2.** TG-MS profiles of the used Ni/m-SiO<sub>2</sub> sample after the initial test of photothermocatalytic steam cellulose reforming with focused UV-vis-IR illumination (a). The yield of char and tar for photothermocatalytic steam cellulose reforming on Ni/m-SiO<sub>2</sub> with focused UV-vis-IR illumination

(b).

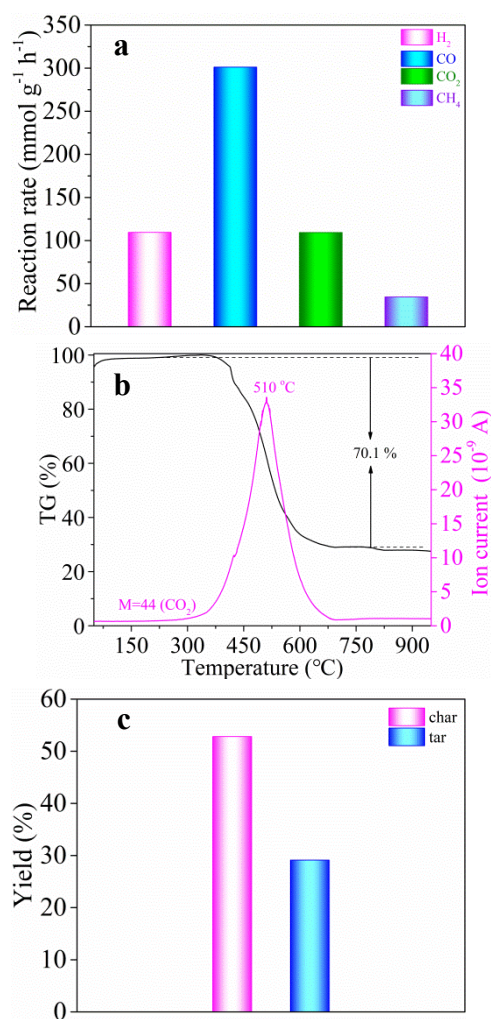


**Figure S3.** The production rates of gases for photothermocatalytic cellulose steam reforming on m-SiO<sub>2</sub> with focused UV-vis-IR illumination (a). TG-MS profiles of the used m-SiO<sub>2</sub> sample after the test of photothermocatalytic steam cellulose reforming with focused UV-vis-IR illumination (b). The yields of char and tar for photothermocatalytic steam cellulose reforming on Ni/m-SiO<sub>2</sub> with focused UV-vis-IR illumination (c)

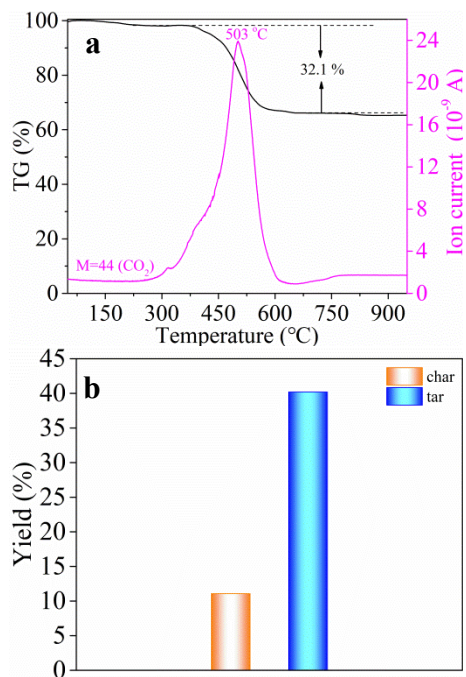


**Figure S4.** TG-MS profiles of the used Ni/m-SiO<sub>2</sub> sample after the test of photothermocatalytic steam cellulose reforming with focused  $\lambda > 420$  nm vis-IR illumination (a). The yield of char and tar for photothermocatalytic steam cellulose reforming on Ni/m-SiO<sub>2</sub> with focused  $\lambda > 420$  nm vis-IR illumination (b).

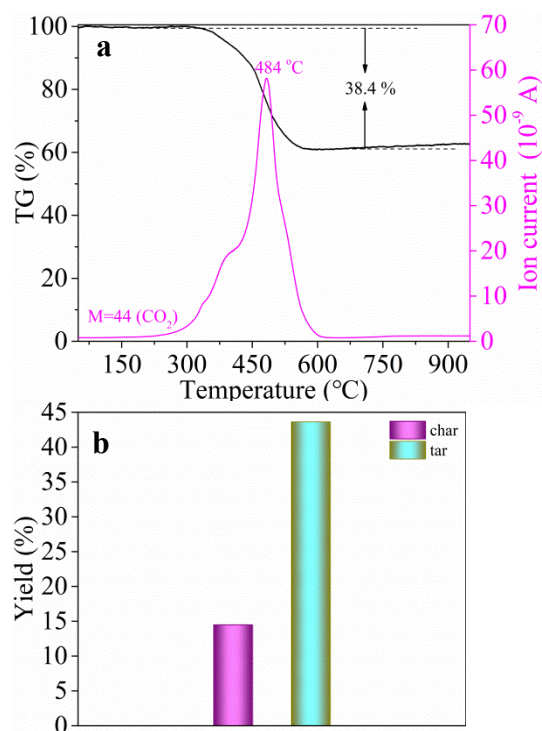


**Figure S5.** TG-MS profiles of the used Ni/m-SiO<sub>2</sub> sample after the test of photothermocatalytic steam cellulose reforming with focused  $\lambda > 560$  nm vis-IR illumination (a). The yield of char and tar for photothermocatalytic steam cellulose reforming on Ni/m-SiO<sub>2</sub> with focused  $\lambda > 560$  nm vis-IR illumination (b).

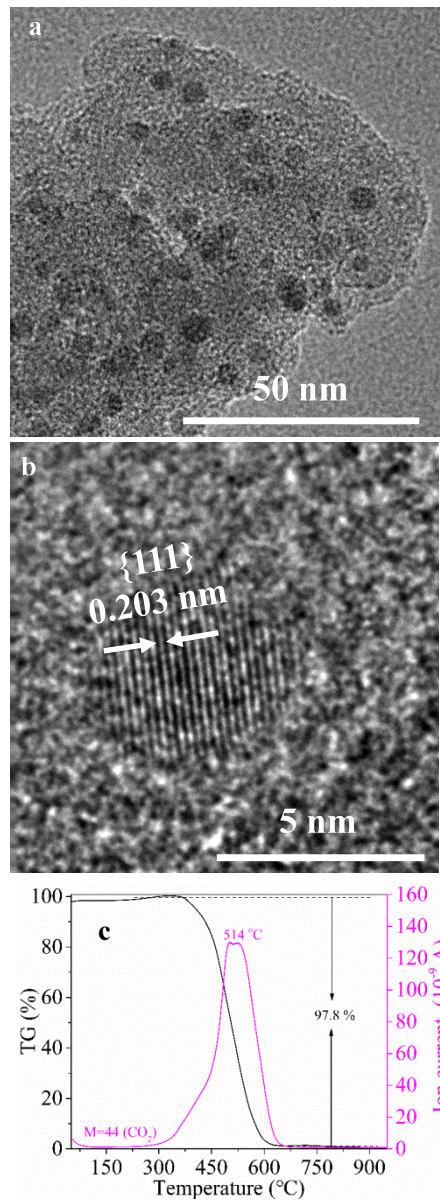


**Figure S6.** TEM image (a), HRTEM (b) image, and TG-MS profiles (c) of the used Ni/m-SiO<sub>2</sub> sample after recycled for four times cycles for photothermocatalytic cellulose steam reforming.

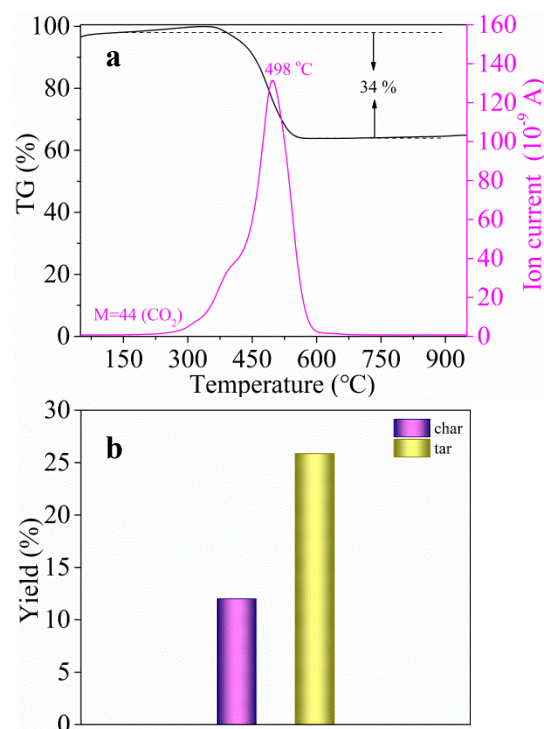


**Figure S7.** TG-MS profiles of the used Ni/m-SiO<sub>2</sub> sample after the test of photothermocatalytic cellulose steam reforming on the regenerated Ni/m-SiO<sub>2</sub> sample with focused UV-vis-IR illumination (a). The yield of char and tar for photothermocatalytic steam cellulose reforming on the regenerated Ni/m-SiO<sub>2</sub> sample with UV-vis-IR illumination (b).

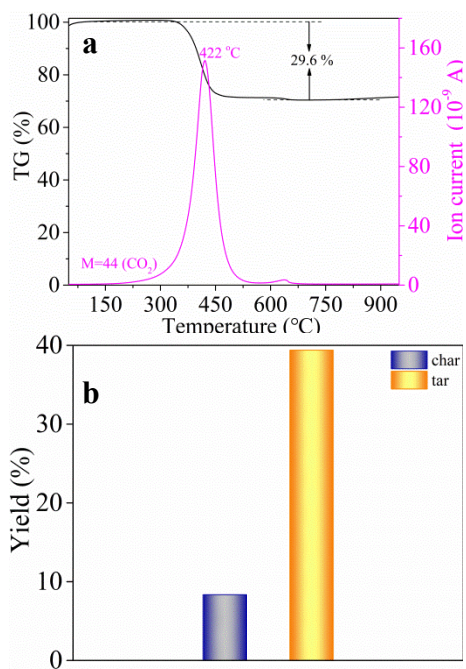


**Figure S8.** TG-MS profiles of the used Ni/m-SiO<sub>2</sub> sample after the test of photothermocatalytic steam reforming of rice straw with focused UV-vis-IR illumination (a). The yield of char and tar for photothermocatalytic steam reforming of rice straw on Ni/m-SiO<sub>2</sub> with focused UV-vis-IR illumination (b).

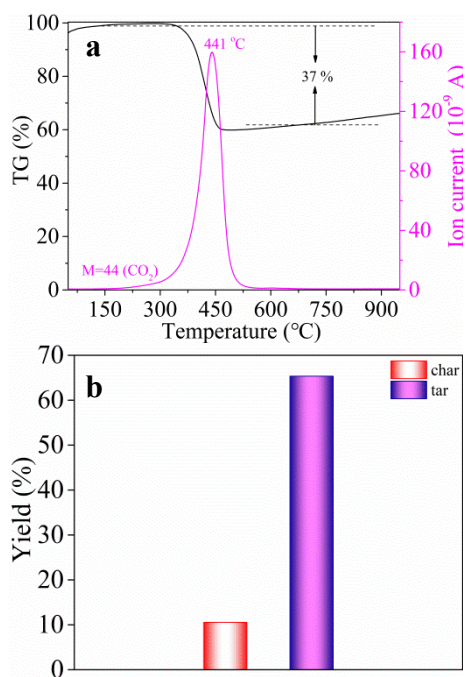


**Figure S9.** TG-MS profiles of the used Ni/m-SiO<sub>2</sub> sample after the test of photothermocatalytic steam reforming of wheat straw with focused UV-vis-IR illumination (a). The yield of char and tar for photothermocatalytic steam reforming of wheat straw on Ni/m-SiO<sub>2</sub> with focused UV-vis-IR illumination (b).

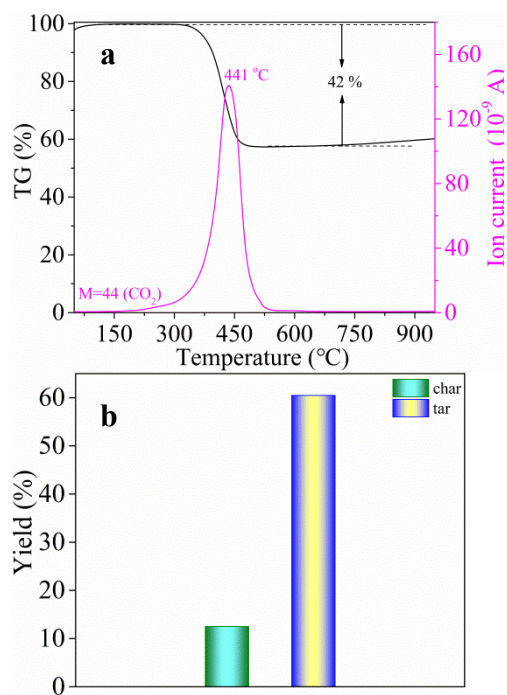


**Figure S10.** TG-MS profiles of the used Ni/m-SiO<sub>2</sub> sample after the test of photothermocatalytic steam reforming of corn stalk with focused UV-vis-IR illumination (a). The yield of char and tar for photothermocatalytic steam reforming of corn stalk on Ni/m-SiO<sub>2</sub> with focused UV-vis-IR illumination (b).

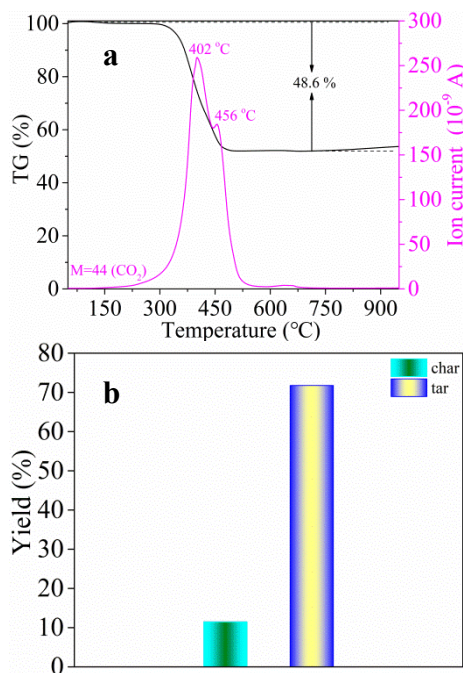


**Figure S11.** TG-MS profiles of the used Ni/m-SiO<sub>2</sub> sample after the test of photothermocatalytic steam reforming of kitchen waste with focused UV-vis-IR illumination (a). The yield of char and tar for photothermocatalytic steam reforming of kitchen waste on Ni/m-SiO<sub>2</sub> with focused UV-vis-IR illumination (b).

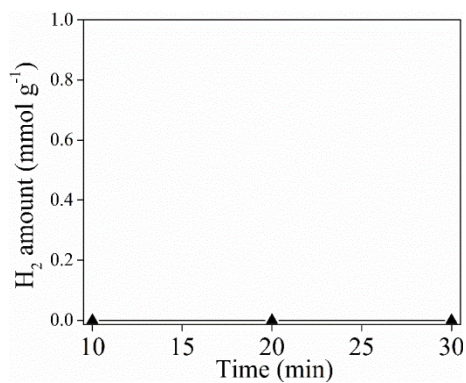


**Figure S12.** Photocatalytic steam cellulose reforming on Ni/m-SiO<sub>2</sub> under focused UV-vis-IR illumination at near room temperature.

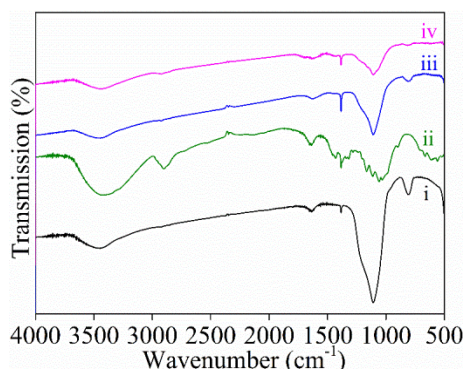


**Figure S13.** FTIR spectra of i) fresh Ni/m-SiO<sub>2</sub>, ii) cellulose, the remained solid mixture after photothermocatalytic steam cellulose reforming on Ni/m-SiO<sub>2</sub> with iii) 0.5 and iv) 3 min of the focused UV-vis-IR illumination.

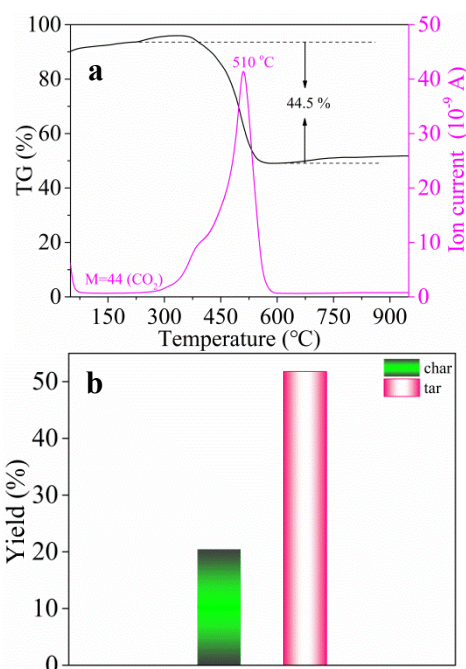


**Figure S14.** TG-MS profiles of the used Ni/m-SiO<sub>2</sub> sample after the initial test of photothermocatalytic cellulose pyrolysis with focused UV-vis-IR illumination (a). The yield of char and tar for photothermocatalytic cellulose pyrolysis on Ni/m-SiO<sub>2</sub> with focused UV-vis-IR illumination (b).

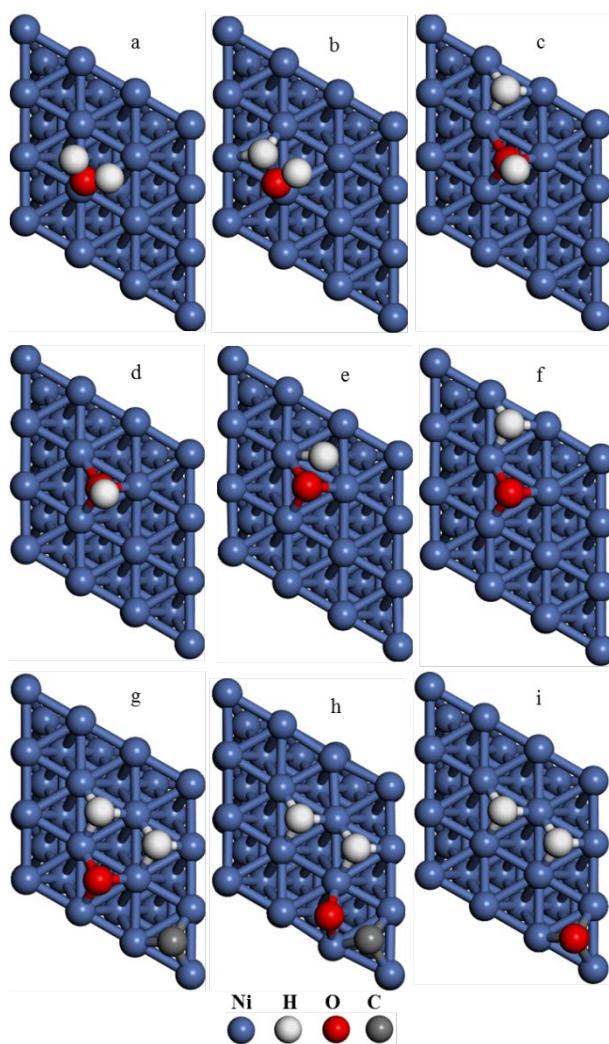


**Figure S15.** The geometries of the initial states, transition states, and intermediates for steam cellulose reforming on the Ni<sub>36</sub> slab in the ground states: (a) chemisorbed H<sub>2</sub>O (A), (b) transition state of H<sub>2</sub>O dissociation, (c) chemisorbed OH and H, (d) chemisorbed OH (A), (e) transition state of OH dissociation, (f) chemisorbed H and O, (g) chemisorbed H, C, and O, (g) chemisorbed H and transition state of C dissociation, and (i) chemisorbed CO and H.

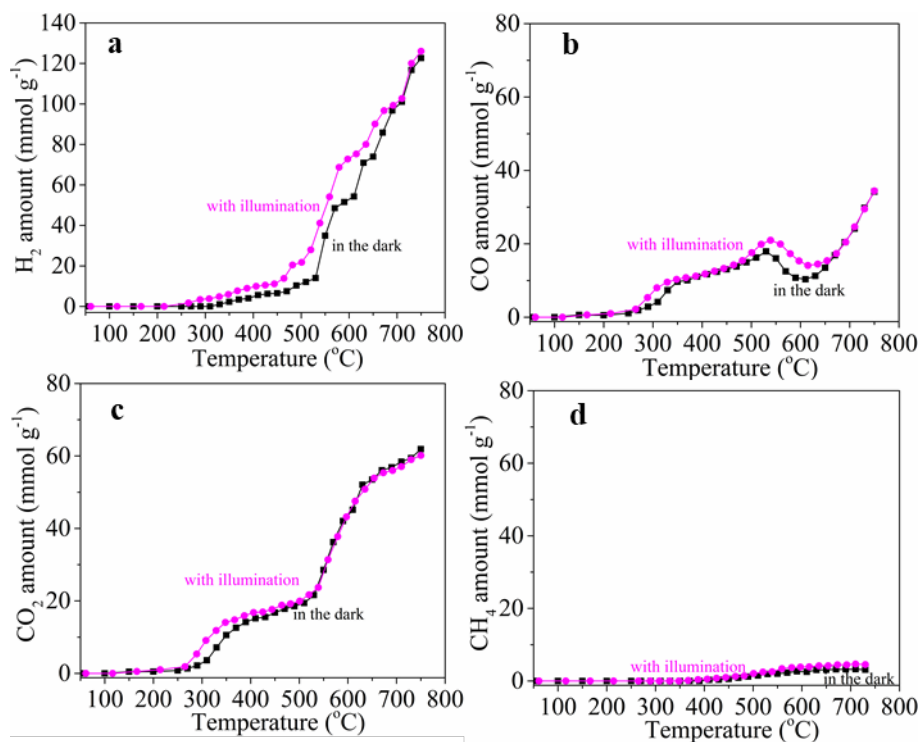


**Figure S16.** The specific amounts of H<sub>2</sub> (a), CO (b), CO<sub>2</sub> (c), CH<sub>4</sub> (d) produced by catalytic cellulose pyrolysis on Ni/m-SiO<sub>2</sub> at different temperatures with focused UV-vis-IR illumination and in the dark.

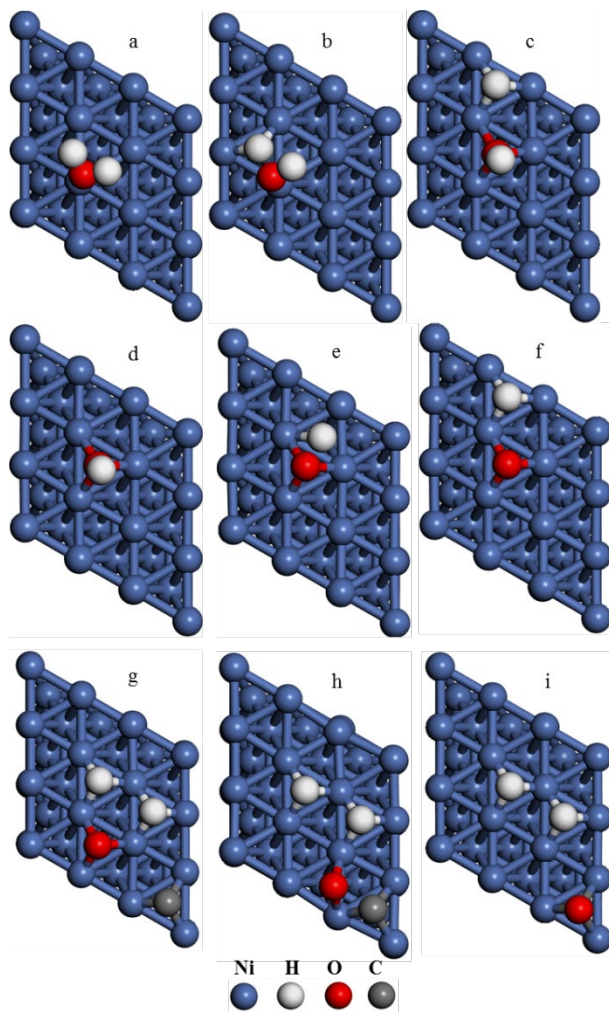


**Figure S17.** The geometries of the initial states, transition states, and intermediates for steam cellulose reforming on the Ni<sub>36</sub> slab in the excited states: (a) chemisorbed H<sub>2</sub>O (A), (b) transition state of H<sub>2</sub>O dissociation, (c) chemisorbed OH and H, (d) chemisorbed OH (A), (e) transition state of OH dissociation, (f) chemisorbed H and O, (g) chemisorbed H, C, and O, (g) chemisorbed H and transition state of C dissociation, and (i) chemisorbed CO and H.

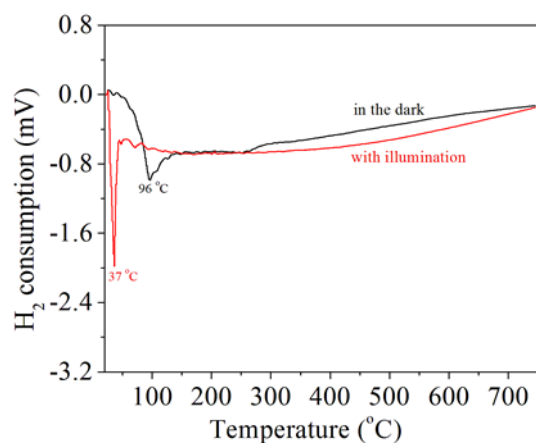


**Figure S18.** TPR profiles of the Ni/m-SiO<sub>2</sub> sample with pre-chemisorbed oxygen on Ni nanoparticles in the dark and with UV-vis-IR illumination.

#### References:

- s1. M. Y. Mao, Q. Zhang, Y. Yang, Y. Z. Li, H. Huang, Z. K. Jiang, Q. Q. Hu, X. J. Zhao, *Green Chem.* 2018, 20, 2857-2869.
- s2. G. Q. Guan, M. Kaewpanha, X. G. Hao, A. Abudula, *Renew. Sustain. Energy Rev.* 2016, 58, 450.
- s3. G. Kresse and J. Hafner, *Phys. Rev. B* 1993, **48**, 13115-13118.
- s4. G. Kresse and D. Joubert, *Phys. Rev. B* 1999, **59**, 1758-1775.
- s5. S. W. Wu, Y. Z. Li, Q. Zhang, Q. Q. Hu, J. C. Wu, C. Y. Zhou and X. J. Zhao, *Adv. Energy Mater.* 2020, **10**, 2002602.
- s6. Yi. A. Zhu, D. Chen, X. G. Zhou and W. K. Yuan, *Catal. Today* 2009, **148**, 260–267.
- s7. D. Sheppard, R. Terrell and G. Henkelman, *J. Chem. Phys.* 2008, **128**, 134106.